ELSEVIER

Physica D 127 (1999) 250–266

PHYSICA D

Nonlinear analyses of interictal EEG map the brain interdependences in human focal epilepsy

Michel Le Van Quyen [a,b,*], Jacques Martinerie [b], Claude Adam [c], Francisco J. Varela [b]

[a] *Höchleistungsrechenzentrum, Forschungzentrum Jülich, D-52425 Jülich, Germany*

[b] *Laboratoire de Neurosciences Cognitives et Imagerie Cérébrale (LENA) (CNRS UPR 640 – University of Paris 6), Hôpital de la Salpêtrière, 47 Bd. de l'Hôpital, 75651 Paris Cedex, France*

[c] *Unité d'Epileptologie, Hôpital de la Salpêtrière, 47, Bd. de l'Hôpital, 75651 Paris Cedex, France*

Received 7 January 1998; received in revised form 11 May 1998; accepted 16 September 1998
Communicated by A.M. Albano

Abstract

The degree of interdependence between intracranial electroencephalographic (EEG) channels was investigated in epileptic patients with temporal lobe seizures during interictal (between seizures) periods. With a novel method to characterize nonlinear cross-predictability, that is, the predictability of one channel using another channel as data base, we demonstrated here a possibility to extract information on the spatio-temporal organization of interactions between multichannel recording sites. This method determines whether two channels contain common activity, and often, whether one channel contains activity induced by the activity of the other channel. In particular, the technique and the comparison with surrogate data demonstrated that transient large-scale nonlinear entrainments by the epileptogenic region can be identified, this with or without epileptic activity. Furthermore, these recurrent activities related with the epileptic foci occurred in well-defined spatio-temporal patterns. This suggests that the epileptogenic region can exhibit very subtle influences on other brain regions during an interictal period and raises the possibility that the cross-predictability analysis of interictal data may be used as a significant aid in locating epileptogenic foci.

Keywords: Temporal lobe epilepsy; Intracranial EEG; Epileptogenic focus; Nonlinear cross-prediction; Surrogate data
PACS: 5.45.+b; 87.10.+e.

1. Introduction

The existence of spatial patterns from neuronal activity is usually studied by mapping amplitudes or spectral powers in a given frequency band [1]. While such topographic maps represent the regional distribution of the neural activities, they do not make full use of the information available in the multivariate data structure corresponding to the interdependences between spatially separated recording sites. This information is essential for understanding how the brain integrates simultaneously distributed and divergent activities into globally coherent patterns [2–4]. In the present paper we propose an approach to study two related questions: (1) When specific patterns of neuronal activities occur simultaneously in two brain regions, do the two regions have close active couplings

* Corresponding author. Address: Laboratoire de Neurosciences Cognitives et Imagerie Cérébrale (LENA-CNRS UPR 640), 47 Bd. de l'Hôpital, 75651 Paris Cedex 13, France. Fax: +33 01 44 243954; e-mail: lenalm@ext.jussieu.fr

0167-2789/99/$ – see front matter
PII: S0167-2789(98)00258-9

with each other, and (2) is one of the two regions the "driving force" of the activities of the other?

The most common methods of studying interactions between several simultaneously recorded neuronal signals are the cross-correlation in the time domain [5], and cross-spectrum (or coherence) in the frequency domain [6] that measure the linear relationship between two variables. Nevertheless, the components of complex extended coupled systems rarely display only linear interdependences. In particular, the complex nonlinear character of the neuronal networks at various levels [7] strongly emphasizes the nonlinear nature of interaction processes. In fact, deviations from linearity are commonly encountered between neuronal recordings [8–10]. Furthermore, the development of techniques for nonlinear analysis has made it possible to investigate the neuronal signals as the realization of a dynamical system of relatively great complexity and containing highly nonlinear elements [11–13]. Indeed, the quantification of the nonlinear structure of neuronal activity was shown to be useful for identifying and characterizing brain states [14–16]. In order to surpass the limitation of linear approaches, more general methods to quantify dynamical interactions have to be developed and applied in electroencephalography. Recently, a method of mutual nonlinear prediction, i.e the prediction of one system based on the knowledge of the other system, was introduced [17] and applied [18] to characterize dynamical interdependences among nonlinear systems. With this method, the components of complex coupled systems were then demonstrated to show mutual interdependences when standard analysis with linear cross-correlation might fail [18].

We focus in this paper on the possibility to use this new nonlinear method to gain some knowledge about the interaction between recording channels of neuronal activity. We have investigated intracranially recorded multichannel electroencephalographic (EEG) obtained from a group of epileptic patients undergoing preoperative evaluation for intractable temporal lobe epilepsy. For these patients, the seizures are thought to originate from a localized region of the brain, the epileptogenic focus, and rapidly propagate to more normal regions. The use of intracranial electrodes provides records which have much better spatial resolution compared to scalp EEG recordings and where the noise and artifact contamination effects are minimized. In practice, electroencephalographers visually inspect the EEG recordings selected to encompass the epileptic seizures and identify the location of the epileptogenic focus as the zone where the seizure is originated. In a different way, the principal objective of the present paper is not to investigate the EEG recordings during seizures but during interictal periods (i.e. between seizures), and ask if the use of nonlinear signal processing techniques provide some valuable information about the epileptogenic regions. Thus, following an earlier study [10], we analyzed the cross-predictabilities between all possible pairs of channels for segments of interictal intracranial EEG recording. We discuss the usefulness of this information in lateralizing and localizing the epileptogenic structures.

The organization of this paper is as follows. In Section 2, we present the nonlinear cross-prediction algorithm and show with numerical examples that this technique can provide some knowledge about the causality between two systems. In Section 3, we describe the intracranial EEG recordings and some computational parameters. In Section 4, we present the results of the cross-predictabilities for several EEG segments and attempt to relate these characterizations to the clinical status of the patient. In Section 5, the clinical and theoretical implications of these results are discussed.

2. Nonlinear cross-predictability

Consider two dynamical systems X and Y in a general sense. The question to be answered is whether we can detect the existence of a functional relation F relating states between the phase spaces $\mathcal{X}$ and $\mathcal{Y}$, i.e.,

$$X \stackrel{?}{=} F(Y).$$

To have an explicit numerical example showing a complicated functional relationship between two systems, we consider the responses of a Lorenz system Y when it is driven by a chaotic signal from a Rössler system X. In our case the drive system X and the response system Y are given by the following equations:

Rössler system X:

$$\dot{x}_1 = -\alpha\{x_2 + x_3\},$$

$$\dot{x}_2 = \alpha\{x_1 + 0.2x_2\},$$

$$\dot{x}_3 = \alpha\{0.2 + x_3(x_1 - 5.7)\},$$

Lorenz system Y:

$$\dot{y}_1 = 10(-y_1 + y_2),$$

$$\dot{y}_2 = 28y_1 - y_2 - y_1y_3 + Cx_2^2,$$

$$\dot{y}_3 = y_1y_2 - 8/3y_3,$$

where C is the strength of the unidirectional coupling and α is introduced to control the characteristic timescale of the driving system ($\alpha = 6$). The perturbation Cx_2^2 is applied only to the second equation of the Lorentz system and does not contain any feedback term. Fig. 1 shows for a strong coupling ($C = 8$) the projection onto the (x_1, x_2) plane of the driving attractor X and the projection onto the (y_1, y_2) plane of the response attractor Y. We can see that the driving severely distorts the trajectory of the Lorenz attractor. The projection onto the (x_1, y_1) plane of the driving-response system is plotted in Fig 1 and indicates that a complex submanifold of the full joint phase space $\mathcal{X} \oplus \mathcal{Y}$ is being occupied. This shows that, for essentially different chaotic systems, the full phase space does not contain any trivial invariant objects to which one can expect a collapse of the overall evolution. Since the relationship between the drive and response dynamical variables are in this case very complicated, the central question is how can we detect the existence of the synchronization condition $X = F(Y)$. A practical algorithm was suggested by Abarbanel et al. [19] based on the fact that if there exists some map F between X and Y then the response system Y becomes a passive system, i.e. it "forgets" its initial conditions. Suppose then that we can construct an auxiliary response system Y' identical with Y and link it to the driving system X in the same way as Y is linked to X. Clearly, when the synchronization $X = F(Y)$ occurs, then the vector fields in the phase spaces of the response and auxiliary systems are identical and the systems evolve on identical attractors. In the case of our numerical example, the functional relationship $X = F(Y)$ can be easily detected with the help of an auxiliary response system. Fig. 2 shows the projections of the response–auxiliary system onto the (y_1, y_1') planes for various values of the coupling strength C. For $C \geq 3$, it can be observed that the synchronization manifolds are projected onto the diagonal $y_1 = y_1'$. Therefore, we can conclude that the drive–response systems are then functionaly related.

Although this auxiliary system method can be easily implemented in the numerical simulations, this method cannot be used in real experimental situations. Recently, Rulkov et al. [17] suggested another approach based on the assumption that F is a smooth map. In fact, if a smooth functional relation exists between the trajectories $\{\boldsymbol{X}_n\}$ in the phase space $\mathcal{X}$ of the driving system X and $\{\boldsymbol{Y}_n\}$ in $\mathcal{Y}$ of the response system Y, this implies that two close states in $\mathcal{X}$ correspond to two close states in the space $\mathcal{Y}$. To exploit this information contained in the point relationships, we can define [17,18] a mutual neighbor $\boldsymbol{X}_j$ of $\mathbf{Y}_i$ as a point in $\mathcal{X}$ that bears the same time index j as some neighbor $\boldsymbol{Y}_j$ of $\boldsymbol{Y}_i$. Similarly, we can define a mutual neighbor $\boldsymbol{Y}_j$ of $\boldsymbol{Y}_i$ in $\mathcal{Y}$. If a function exists that maps the values $\boldsymbol{X}_i$ to $\boldsymbol{Y}_i$, this further implies the ability to predict the next state of $\boldsymbol{Y}_i$ by its mutual nearest neighbors. Let us fix a length scale ϵ. For each $\boldsymbol{Y}_n$, we want to make a one-step prediction of one component Y_{n+1} of $\boldsymbol{Y}_{n+1}$ using the mutual neighbors in $\mathcal{X}$. We may define

$$\hat{Y}_{n+1} = \frac{1}{|V_\epsilon(\boldsymbol{X}_n)|} \sum_{j\,:\,\boldsymbol{X}_j \in V_\epsilon(\boldsymbol{X}_n)} Y_{j+1},$$

where $V_\epsilon(\boldsymbol{X}_n) = \{\boldsymbol{X}_{n'} : |\boldsymbol{X}_{n'} - \boldsymbol{X}_n|) < \epsilon\}$ is an ϵ-neighborhood of $\boldsymbol{X}_n$. $|V_\epsilon(\boldsymbol{X}_n)|$ denotes the number of elements in that neighborhood. The cross-predictability is then defined as 1 minus the root mean square prediction error [1]:

$$\mathrm{Pred}_{X\to Y} = 1 - \sqrt{\frac{1}{N}\sum_{n=1}^{N}(\hat{Y}_{n+1} - Y_{n+1})^2}.$$

Let us illustrate the method of cross-predictability with the previous numerical example of a Lorenz system driven by a Rössler system. We used a neighborhood of radius $\epsilon = 0.2$ (at unit root mean square amplitude) and several segments of length $N = 4096$ for different values of the coupling C. Fig. 2 shows the results of the mutual nonlinear cross-predictabilities versus the strength of coupling coefficient C (varying from $0 \to 9$). One can see that the predictibilities $\mathrm{Pred}_{X\to Y}$

[1] Note that this statistical test is different from other cross-prediction algorithms which evaluate the closeness between two attractors [31–33]. We investigate here the existence of a mapping between the trajectories of two attractors. See Section 5.

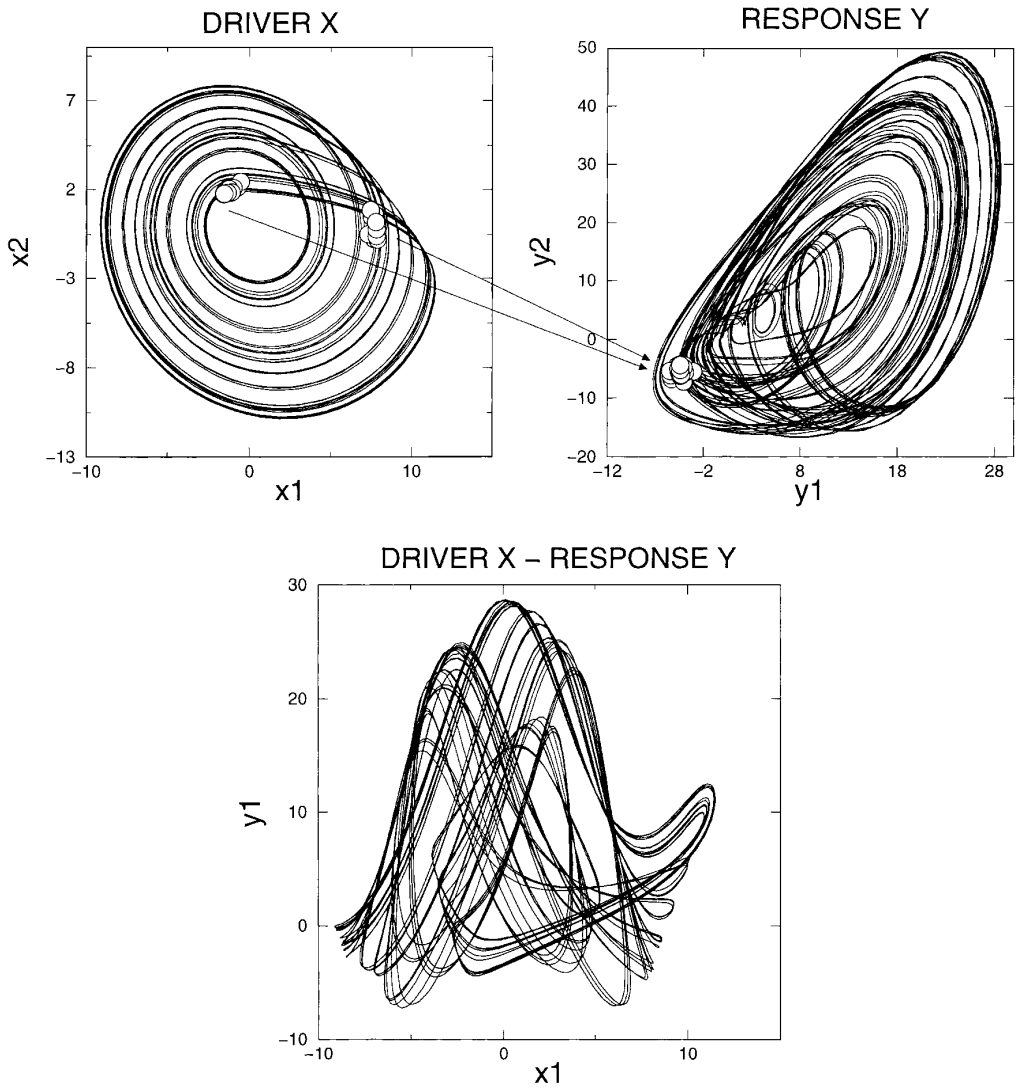

Fig. 1. *Top:* The projections of the original Lorentz attractor (driver X) and driven Lorentz attractor (response Y). The coupling parameter is $C = 8$ and the systems are coupled as indicated in the text. Note that neighbor points in the phase space of Y (circles) are not always neighbors in the phase space of X characterized by the same time index. Indeed, the noninjectivity of the mapping between X and Y induces that separate parts of the phase space of X are glued together. *Bottom:* The projection of the coupled dynamics X vs Y shows that a complex submanifold of the full joint plane is occupied.

increase monotonically with C and that a strong level dynamical relationship is reached for $C \approx 3$.

Interestingly, we can further observe that the mutual nonlinear predictabilities are asymmetric $\mathrm{Pred}_{X\to Y} > \mathrm{Pred}_{Y\to X}$, particularly at strong levels of the coupling. This can be explained taking into consideration that Y is a single-valued function of X, but X is not a single-valued function of Y (e.g. no injectivity, see arrows in Fig. 1) which means that Y does not contain enough information to predict all points in X [20]. This is an important property because an investigation of the degree of symmetry can give insight into the nature of the relationship between two systems. In particular, in our specific situation where a subsystem X drives another one Y without being strongly influenced by the latter, the crucial feature of the relationship is the abil-

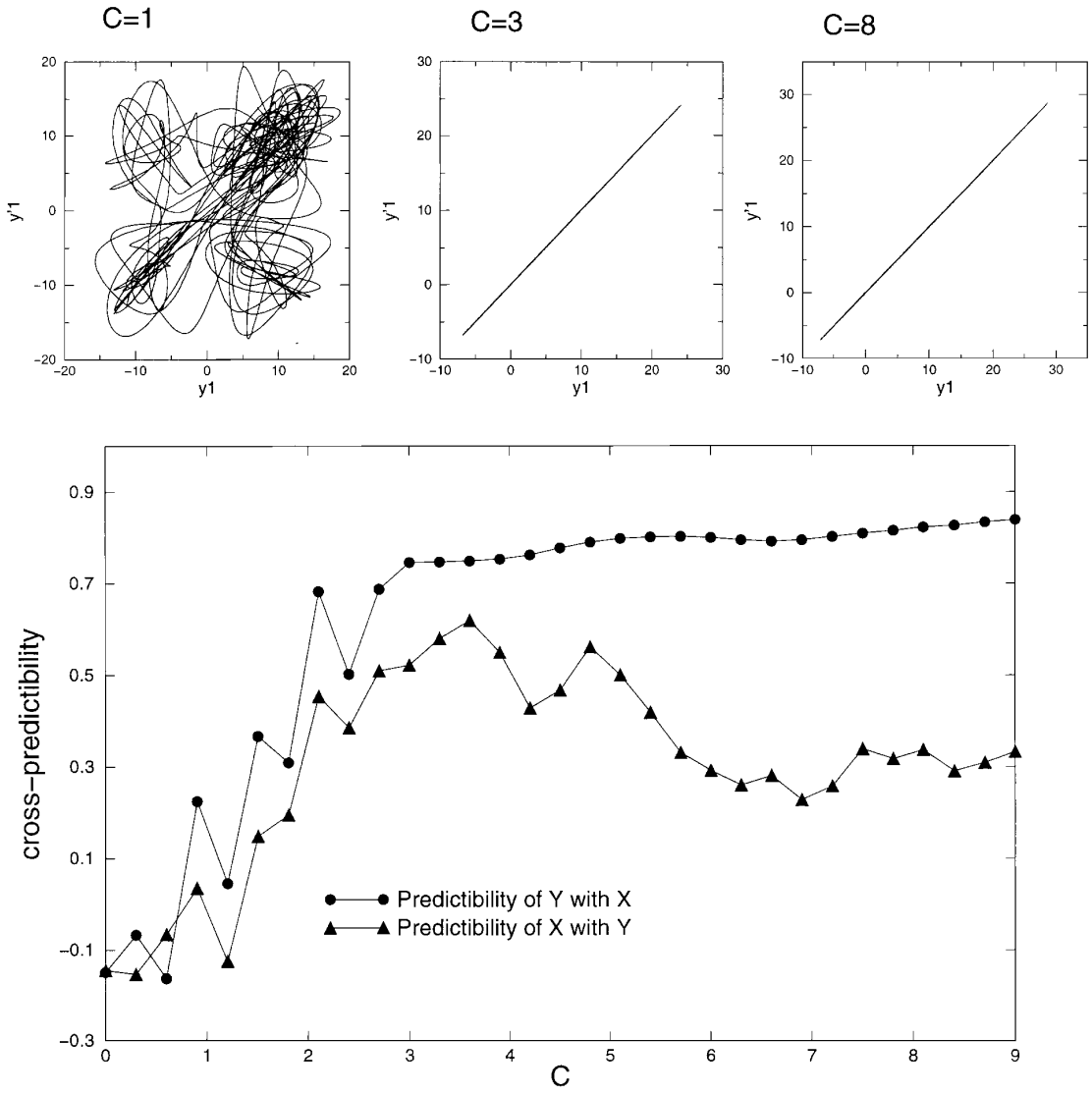

Fig. 2. *Top:* For several coupling strengths, projections of the state space of the response-auxiliary system from which the stability of the functional relationship between the drive–response system follows. For $C \geq 3$, it can be observed that the synchronization manifolds are projected onto the diagonal $y_1 = y_1'$. Therefore, we can conclude that the drive–response systems are then functionaly related. *Bottom:* Cross-predictabilities between the system X and Y vs. the coupling parameter C. Note the asymmetry in the cross-predictabilities of Y using X and X using Y due to the fact that the mapping between X and Y are not injective.

ity to predict the response Y from observation of the driver X alone [17,21]. Therefore, it can be assumed that each state Y is necessarily a single-valued function of X, but each state of X is not always a single-valued function of Y. In this case, a large asymmetry $\mathrm{Pred}_{X\to Y} \gg \mathrm{Pred}_{Y\to X}$ provides a strong evidence of unidirectional interaction $X \to Y$, where the system X has a strong contribution in the activities Y.

3. Experimental setup

Temporal lobe epilepsies are the most predominant medically intractable epilepsies and patients suffering from these refractory epilepsies are more frequently considered for surgical treatment [22]. Epilepsy surgery requires then the exact delineation and localization of the epileptogenic zone (i.e. the

brain area that generates the seizure). Consequently, intracranial recordings of continuous depth EEG activity by chronic multi-contact electrodes are sometimes needed to locate this epileptogenic "focus". For the patients investigated here, two depth electrodes, insulated wires with eight contacts (of 1 mm diameter and 8 mm apart), were inserted stereotaxically under MRI control along a posterior trajectory to sample the mediotemporal and occipital cortical structures (see bottom of Fig. 3). Additional intracerebral or subdural electrodes with eight contacts 1 cm apart were added to explore the other suspected cortical structures (see top of Fig. 3). The raw data were passed to a 32-channel amplifier system with band-pass filter settings of 0.5–99 Hz using an external reference over linked ears. The data recordings were digitized at a rate of 200 Hz, with 12 bit resolution. For this study, we selected a group of four patients. Their seizures originated unilaterally from mesial structures of the temporal lobe. According to a visual assessment of the recording, we took long-duration artifact-free EEG samples during interictal periods (at several hours from a seizure). The patients were awake in bed, watching television. Regarding the temporal characteristics, the EEG signals are intrinsically non-stationary phenomena. Nevertheless, the recordings can be subdivided into short epochs where the stationarity hypothesis is nearly accomplished. The EEG recordings were here divided into adjacent segments of 5.12 s ($N = 1024$ pts) duration. Segmentation of the same order of magnitude has been used by others [12,15,23]. Fig. 4 (patient 1) illustrates different EEG segments regarded as quasi-stationary and selected for subsequent quantitative analyses presented in this paper.

Let the EEG voltage measurements of a given electrode be denoted by v_i ($i = 1, \ldots, N$). Each time series will be normalized to unit variance and zero mean. Using the method of time delay embedding, we can reconstruct a trajectory $\{\boldsymbol{x}_i\}$ in a D-dimensional space using D measurements with an appropriately chosen time lag τ,

$$\boldsymbol{x}_i = (v_i, v_{i-\tau}, \ldots, v_{i-(D-1)\tau}).$$

For each of the EEG segments, an optimal time lag τ was defined by a reconstruction expansion technique [24]. To determine the number D of coordinates required to unfold the dynamics, one examines the num-

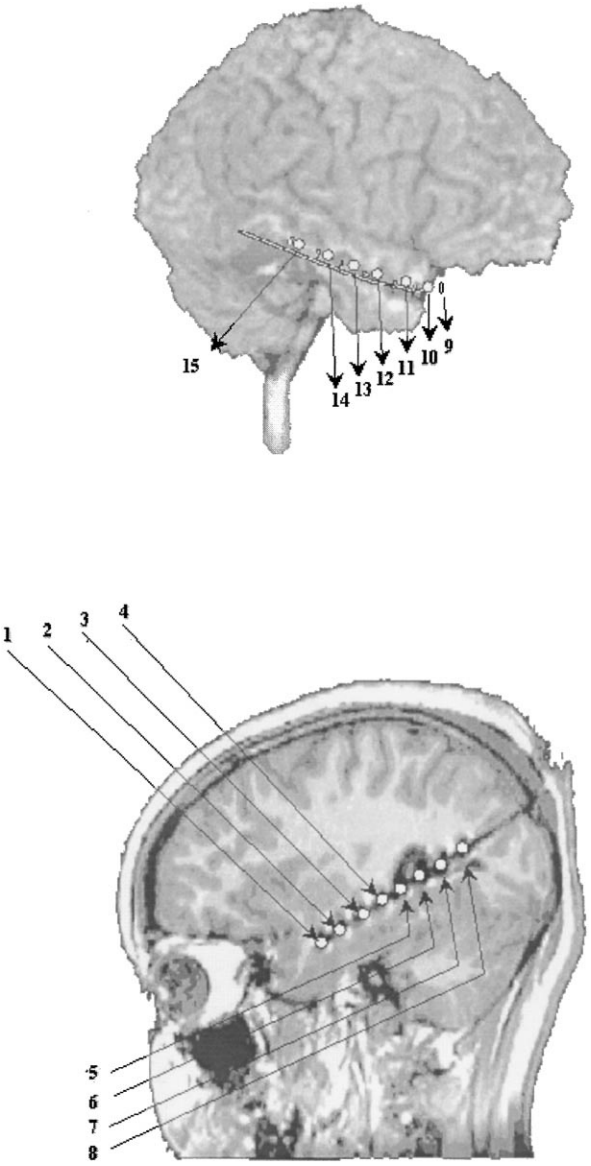

Fig. 3. Usual MRI locations of two intracranial electrodes in the right temporal lobe. *Bottom:* The depth electrode has four contacts (1–4) in the medial temporal structures (amygdala and hippocampus), four contacts in the temporo-occipital junction (5–6) and the lateral occipital cortex (7–8). *Top:* The subdural temporal electrode explores the external temporal neocortex along the long axis of the temporal lobe (9–15). Other subdural and intracerebral electrodes are usually placed in other sites (not shown). The size of the contacts is highly magnified here and is in reality 1 mm wide.

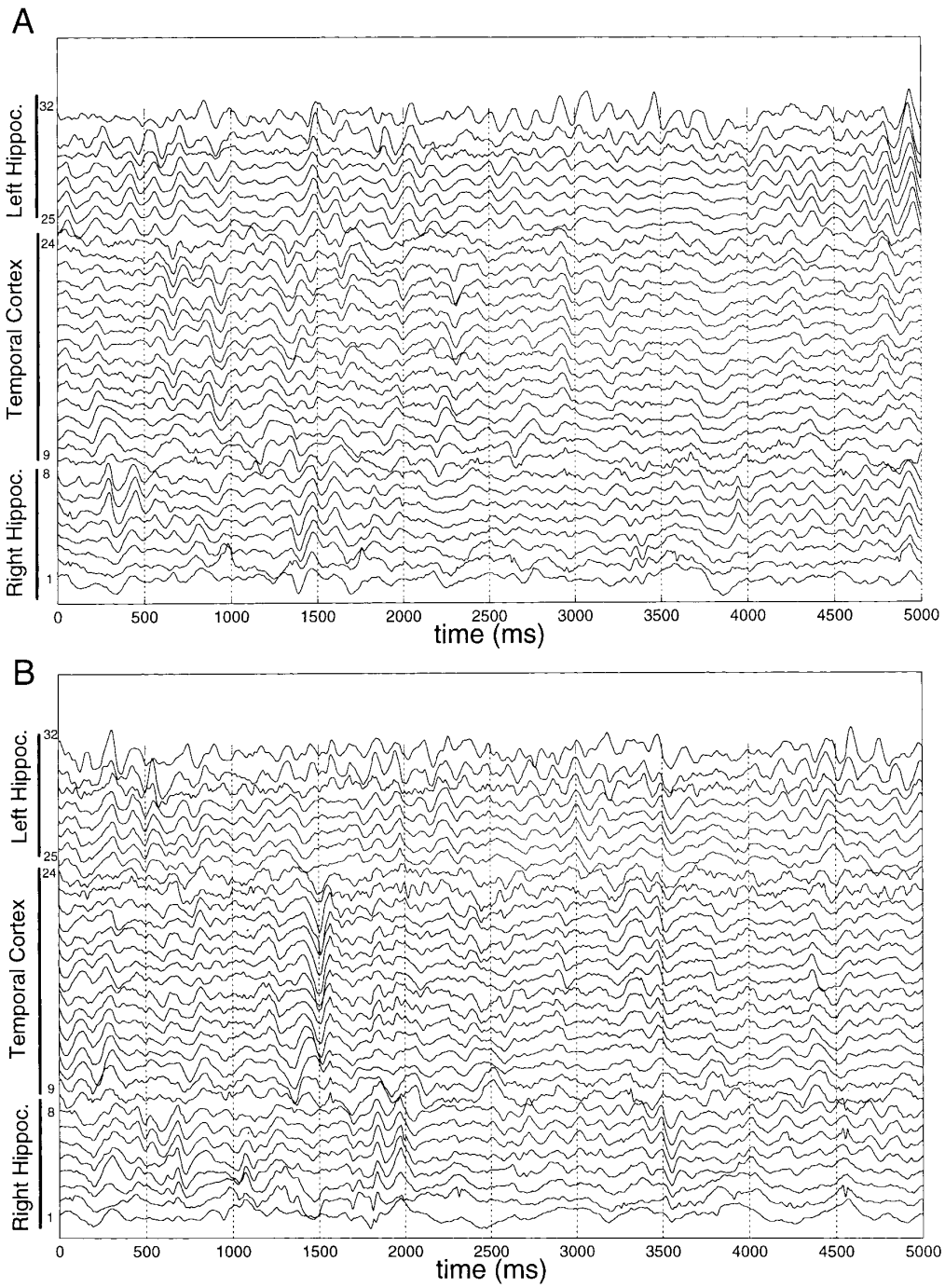

Fig. 4. Two distinct 32-channel EEG segments of 5.12 s duration recorded from patient 1 during an interictal period. Note that no clear epileptic activities are present. The denomination "Hippoc." in the figure actually describes the amygdalo-hippocampal complex defined by the amygdala (right: channel 1 and left: channel 25) and hippocampus (right: channels 2–6 and left: channels 26–30).

ber of self-crossings of the trajectories in the reconstructed state space by the method of false nearest neighbors [25]. The idea behind this test is to check whether nearest neighbors in the reconstructed state space are neighbors due to the dynamics or rather due to the projection of the original state space into a space of inappropriately low dimension. To this end, one looks for nearest neigbors in a d-dimensional space and calculates the distance of these points in a $(d + 1)$-dimensional space. If the distance in the higher-dimensional space is very large, we have found a false nearest neighbor (FNN) since the two points are close in d dimensions only due to the too low-dimensional projection. The percentage of FNN over all pair of neighbors tested should go to zero when we have found a good embedding. We analyzed several EEG channels and segments with this algorithm (threshold sizes of $R_{\text{tol}} = 10$ and $A_{\text{tol}} = 2$, see [25] for details). In most cases, there is a sharp drop to zero at dimension 4–5 after which the percentage of FNN remains small (around 5 %). This provides suggestive evidence that the dimension 4–5 is able to capture most of the EEG dynamics and that additional dimensions for the data space may not be required. Furthermore, recent work has shown that accurate prediction based on the reconstructed self-intersecting attractor is possible for small enough size of neighborhood [26]. This result might justify modeling of the EEG dynamics in a low-dimensional space which permits to use a sufficient computation speed. In conclusion, an embedding dimension of 4 was used for the subsequent computations in this paper and is also consistent with other studies [12,23].

4. Cross-predictability between EEG signals

For each selected time window, the nonlinear mutual predictabilities were determined between all possible pairs of channels. The neigborood radius ϵ is chosen to be 0.1 (at unit rms amplitude) as other studies [12,13] to retain benefits of computational speed. Fig. 5(A) illustrates for the window depicted in Fig. 4(A) the matrix of nonlinear cross-predictibilities between all the pairs of the 32 channels. For this patient, the most anterior contacts of the depth electrodes were in the amygdala (numbered 1 for the right electrode and 25 for the left electrode), the next three in

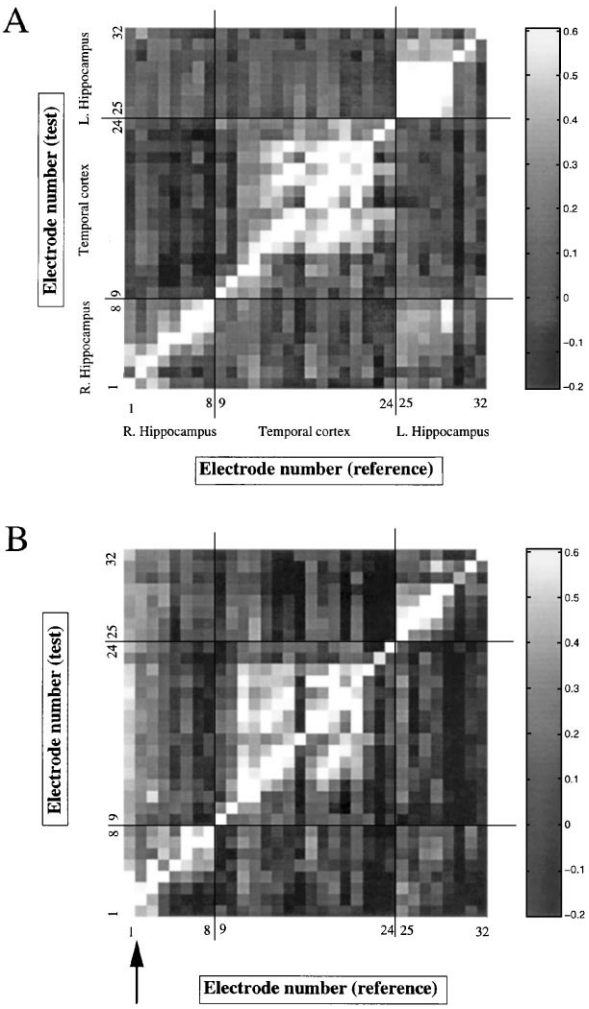

Fig. 5. The nonlinear cross-predictability matrices between all the pairs of the 32 EEG channels estimated for the two segments A and B of Fig. 4 (patient 1). Note the high cross-predictabilities values throughout the entire column above the channels 1–4 (arrow) in the matrix for B. The denomination "Hippocampus" in the figure actually describes the amygdalo-hippocampal complex defined by the amygdala (right: channel 1 and left: channel 25) and hippocampus (right: channels 2–6 and left: channels 26–30).

the hippocampus (numbered 2–4 and 26–28) and the last few in the temporo-occipital junction or lateral occipital cortex (numbered 5–8 and 29–32). Other subdural electrodes (channels 9–24) were placed on the temporal neocortex either basal or external. This patient presented an epileptogenic area in the right hippocampus. In Fig. 5 the predictabilities are encoded as linear gray scales. The examination of the column above each channel on the origin axis reveals the pre-

dictability of all channels (test) using the given channel as data base (reference). A bright value indicates that two channels contain a common pattern of activity. The examination of the matrix in Fig. 5(A) indicates that the various anatomical structures (right, left amygdalo-hippocampal complex, and neocortex) reflected strong degrees of internal interactions. These interdependences decline with the distance, and distinct anatomical regions are only weakly interdependent. However, a slight interdependence between the two hippocampi can be seen. Interestingly, differences in the interaction patterns within each region can be observed: the interdependencies between the adjacent channels in the neocortical structures (central region of the matrix) often reveal local discontinuities, and show, over large domains, a mosaic of local high and low interactive patches. In addition, the analysis of successive windows shows that the interactions between cortical networks are highly variable in time. On the contrary, the interdependencies in each amygdalo–hippocampal complex reveal a spatial homogeneous and more temporally stable distribution of the interactions. There are also differences between left and right mediotemporal structures: the interdependencies in the left non-epileptogenic amygdalo–hippocampal complex (channels 25–28) demonstrated more stronger and distributed patterns of functional interactions than the homologous epileptogenic contralateral structures (channels 1–4).

Other significant dissimilarities between the two hippocampi was the transient occurrence of distant interactions originating from the epileptogenic region. An example is given by the cross-predictability matrix of Fig. 5(B) corresponding to the window shown in Fig. 4(B). In this figure, signals from specific electrodes exhibit strong cross-predictabilities throughout the entire column above their locations in the matrix. Here the most prominant effects are generated by the first channel in the amygdala and the adjacent ones located in the right hippocampus.

As previously commented, the asymmetry of the cross-predictability matrix can provide valuable insights into the direction of relationship between two systems. Here, an investigation of the degree of symmetry shows that $\mathrm{Pred}_{C_i \to C_j} \gg \mathrm{Pred}_{C_j \to C_i}$ for i =1–4 and j =1–32. These asymmetries can be better visualized in Fig. 6(B) where the matrix of the differences $\gamma_{i,j} = \mathrm{Pred}_{C_i \to C_j} - \mathrm{Pred}_{C_j \to C_i}$ are plotted. Indeed, prominent values for i =1–4 was clearly

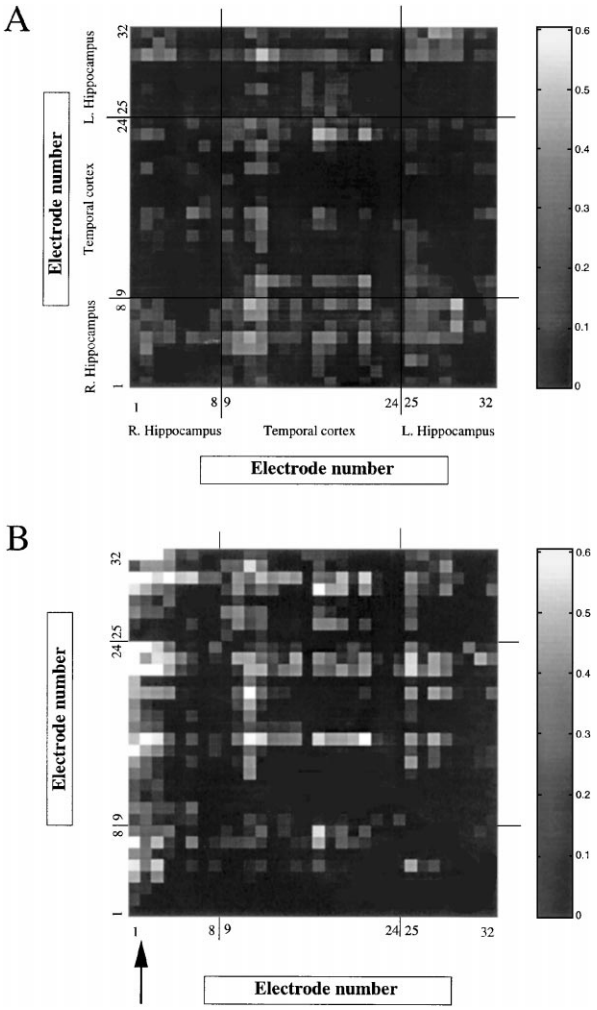

Fig. 6. Matrix of the differences ($\gamma_{i,j} = \mathrm{Pred}_{C_i \to C_j} - \mathrm{Pred}_{C_j \to C_i}$) for the two EEG segments A and B of Fig. 4. The arrow in B indicates the existence of a strong asymmetry for the channels 1–4.

apparent for this segment (data B in Fig. 4). Furthermore, the difference matrix of the cross-predictability for the first segment (data A in Fig. 4) is similarly depicted in Fig. 6(A) and shows in this case no clear asymmetry patterns.

As pointed out before, the strong asymmetrical cross-prediction patterns suggest driving effects. In our case (data B), specific sources in the right amygdala (channel 1) and hippocampal structures (at channels 2–4) transiently appear as predominant driving activities of large portions of the brain. We have not discerned comparable strong interactions from the contralateral channels 25–28. Moreover, the

comparison between these locations and the results of presurgical evaluation confirmed that these sources are in the epileptogenic area generating the seizures. Thus, this phenomenon demonstrates that widespread entrainments of brain activities by the abnormal epileptogenic structures were present even during the interictal period. In particular, single generators could be localized as primarily responsible for these entrainments (here the first four channels in the case of the patient 1). Moreover, no prominent epileptiform activities (like interictal spikes) were present in the EEG segment under examination. This suggests that the epileptogenic region can exhibit very subtle influences on other brain regions even during an interictal period without epileptic activity and that the cross-prediction algorithms used in this paper give a detailed characterization of these effects.

The nonlinear cross-predictabilities may indicate interactions that the linear methods could not account for. To investigate whether the multichannel time series involve nonlinear structures, we use here the technique of surrogate data [27,28]. For several multichannel EEG segments, we generated artificial signals which will preserve both the autocorrelations of each time series and the cross-correlation between them, but nonlinear relationships between channels are lost. Fig. 7(B1) shows the matrix of cross-predictabilities for one surrogate set computed for the same EEG segment as in Fig. 5(B). These two matrices can then be compared to characterize the nonlinear phenomena. In the matrix of the surrogate datasets, the local interactions between anatomical structures demonstrate a high degree of coupling, especially on the left-hand side and to a less degree on the right epileptogenic side. These results were globally similar to those found in the original data, and indicate that the nature of the local functional links are mostly linear. It can be further seen that the differences between original and surrogate computation was most apparent in the interdependencies between distant structures. In particular, the strong widespread cross-predictabilities from the epileptogenic sources identified in the original data can no more be established in the surrogate data set. Furthermore, no asymmetries can be seen in the matrix. The presence of these differences suggests that the process of the large-scale entrainment induced by the epileptogenic regions most likely involves nonlinear functional couplings between neuronal sources.

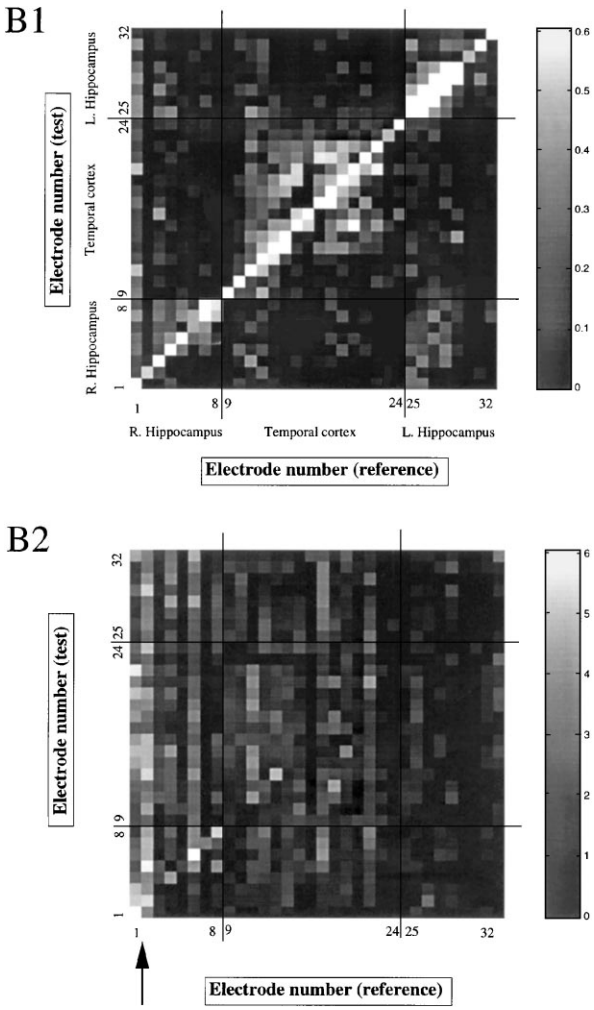

Fig. 7. (B1) Cross-predictability matrix for one surrogate set of EEG segment B (Fig. 4). Strong and asymmetric cross-predictabilities generated by the channels 1–4 can not be observed. (B2) Matrix of nonlinear significance for the same segment. Note the high significance values throughout the entire column above the channels 1–4 (arrow) in the matrix. $S > 3$ is here in gray colored.

A precise estimation of the statistical significance of nonlinear structures was defined as follows [27,12,13]: 19 surrogate data sets for several multichannel EEG segments were generated. The predictions of time series between k and l ($k, l = 1, 32$) were calculated for the original time series and the surrogate time series, i.e. $\mathrm{Pred}^{\mathrm{raw}}_{k,l}$ and $\mathrm{Pred}^{\mathrm{sur}}_{k,l}$. Let $\langle \mathrm{Pred}^{\mathrm{sur}}_{k,l} \rangle$ and $\mathrm{SD}^{\mathrm{sur}}_{k,l}$ denote the mean and the standard deviation of the distribution of the surrogate predictabilities. The measure

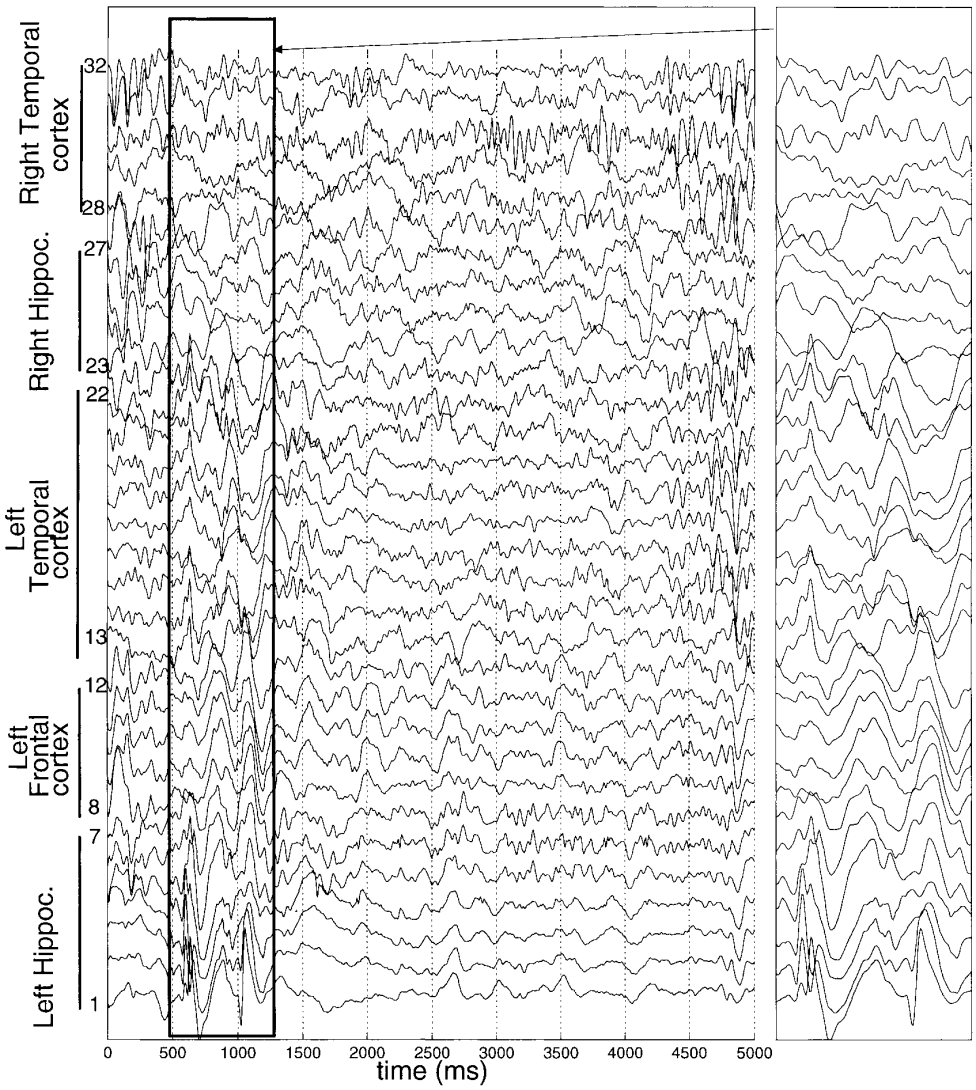

Fig. 8. One 32-channel EEG segment of 5.12 s duration recorded from patient 2 during an interictal activity. The window shows that a clear epileptiform potential (spike) is present in most of channels. An examination suggests that this pattern originated from channels 1–4 and spread to other distant channels.

of significance S was then defined by the difference between the original and the mean surrogate value, devised by the standard deviation of the surrogate values:

$$S_{k,l} = \frac{\mathrm{Pred}^{\mathrm{raw}}_{k,l} - \langle \mathrm{Pred}^{\mathrm{sur}}_{k,l} \rangle}{\mathrm{SD}^{\mathrm{sur}}_{k,l}}$$

A significance S greater than 3 represents at least a 3 standard deviations effect, and indicates then a significant difference between $\mathrm{Pred}^{\mathrm{raw}}$ and $\langle \mathrm{Pred}^{\mathrm{sur}} \rangle$ at the $p = \mathrm{erfc}(S/\sqrt{2}) = 0.05$ level [27]. This level is considered here as statistically significant for nonlinear interdependencies. If the significance is lower, the original and the surrogate data are identical in the sense that both can be well described by a linear model. Fig. 7(B2) shows the matrix of nonlinear significance $\{S_{k,l}\}_{k,l=1,32}$ computed for the segment B of Fig. 4. Any gray value indicates a significance S greater than 3 and shows that the corresponding coupling is nonlinear. In a consistent way with the previous observa-

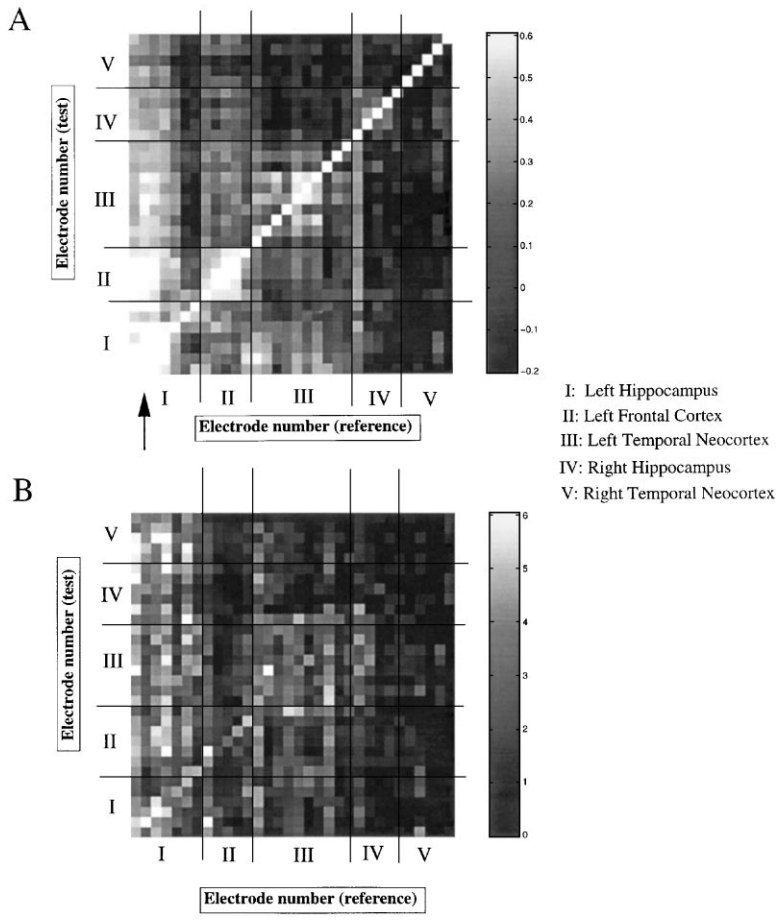

Fig. 9. (A) Cross-predictability matrix between all the pairs of EEG channels for the time segment of Fig 8. (B) Matrix of nonlinear significance for the same segment.

tions, the matrix indicates that most of the significant nonlinear couplings are induced by the epileptogenic region (channels 1 and 2).

Comparable results were obtained in the EEG recordings of another patient (patient 2). The placement of the multicontact electrodes was similar as previously (see Fig. 8), and the clinical analysis of the seizure recordings indicated for this patient an epileptogenic focus in the left temporal structure. In Fig. 8, we display a particular time segment of the EEG signals where interictal epileptiform activity was present (see arrow in the selected window). According to the visual clinical analysis, those infrequent, morphologically variable transient patterns (e.g. sharp waves, spikes, spikes and slow waves) present in many channels are associated with the epileptogenesis and give often partial insights in the spatial spread of epileptiform activity. The clinical assessment of the spike of Fig. 8 by an electroencephalographer (CA) showed that this event seems to originate from sources at the channels 1–4 in the left hippocampus and propagate to the corresponding neocortex, but not to the right-hand side of the hemisphere. The presurgical evaluation confirmed that the sites 1–4 are the leading generators during seizures.

Fig. 9(A) shows the corresponding cross-predictability matrix. Note that the segment under consideration is strongly nonstationary. Nevertheless, the localizations of high values and their clear asymmetry confirm the presence of widespread driving activities by the first channels 1–4 (left amygdala–hippocampus), and to a lesser degree, other cortical

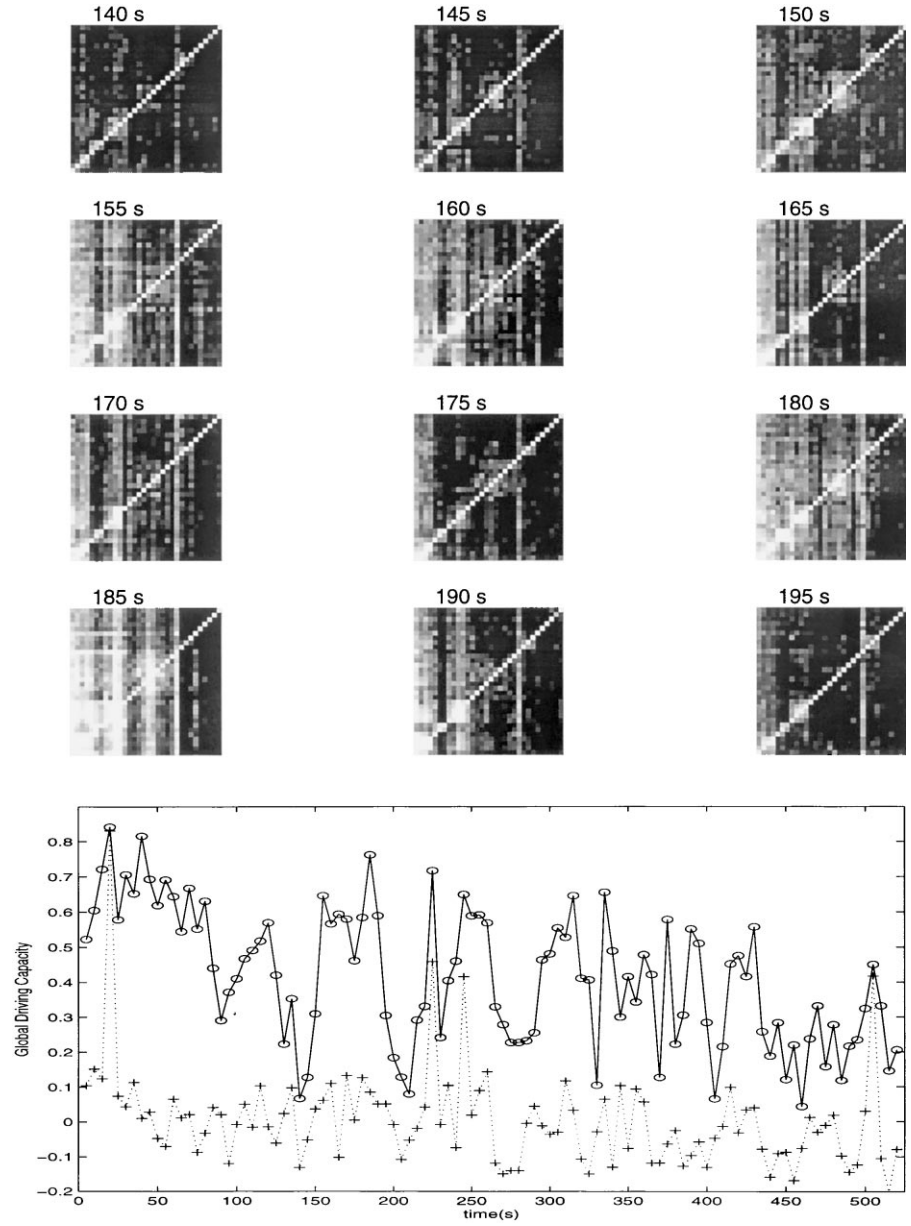

Fig. 10. *Top*: Several cross-predictability matrix of successive EEG segments from patient 2. *Bottom*: *Solid line with circles* – Time course of the global driving capacity of the left epileptogenic region (channels 1–4) and *Dotted line with crosses* – Time course of the global driving capacity of right contralateral regions (channels 23–26).

channels (in particular 8–12 in the left frontal cortex). Thus, the result of the cross-predictabilities was in good agreement with the visual clinical interpretation of the EEG tracings and detected further interactions not suspected on the naked EEG (like the distant drivings by the left epileptogenic structure of the hippocampus and temporal neocortex in the right hemisphere). Fig. 9(B) shows the corresponding nonlinear significance matrix and here, again, these significances clearly demonstrate the strong nonlinear character of the epileptiform phenomena. Several cross-predictability matrices of successive EEG seg-

ments from patient 2 are shown in Fig. 10. The visual inspection revealed that the focal entrainments of channels 1–4 and other adjacent channels were going in and out in an intermittent manner. In order to quantify the degree of this large-scale entrainment of brain activity by one region R, we can define the global driving capacity Δ_R of region R as the mean cross-predictabilities of the p recording channels C_i located in R predicting all other channels:

$$\Delta_R = \frac{1}{p}\sum_{C_i \in R}\frac{1}{N-1}\sum_{j\neq i}\mathrm{Pred}_{C_i \to C_j},$$

where N is the total number of channels. In the bottom of Fig. 8, we display the time course during 9 minutes of the global driving capacity of the left epileptogenic region (the amygdala and hippocampus) and the right contralateral region. It can be observed that the frequent entrainments by the right hippocampal derivations are uniformly higher than for the left hippocampal channels. For this patient the durations of the most prominent magnitudes were widely distributed from 5 to 60 s and visually evidenced no clear temporal structures. A precise analysis of these evolutions is under investigation.

Further comparable observations for the other patients of the defined group confirm our principal result. Indeed, recurrent nonlinear entrainments were frequently observed and their generators can be precisely located in the hemisphere of the brain where the epileptogenic region is situated. This localization for a given patient and electrode are remarkably stable. In contrast, there is considerable variation among different patients, this consistently with the clinical diagnoses. Again, these phenomena can be observed in EEG recordings which do not contain a clear epileptiform activity. We conclude that the nonlinear prediction techniques gives a picture about the spatio-temporal patterns during the interictal period which can be very useful for the localization of the epileptogenic foci and the characterization of epileptiform propagation patterns.

5. Conclusions

The principal result of our work demontrates that the nonlinear cross-prediction technique can be used to measure the degree of interdependence between EEG channels, so that physiologically meaningful interpretations can be made. This suggests that the presented method, already successfully used for studying small in vitro neuronal ensembles [18], can be readily extended to large-scale study of the cerebral cortex. We showed that this method can be used for the determination of synchronizations between the activities from different electrode sites. This determination may be useful to help to understand how widely distributed neuronal ensembles can be engaged in a global and large-scale dynamics [36]. In fact, the high degree of reciprocal interconnections in the brain makes it reasonable to look for synchronous phenomena and their specific topographic characteristics. Several linear methods have been used with this aim. Here the nonlinear cross-prediction allows one to take a much broader view of synchrony than pure linear couplings which could also be used in situation where the EEG signals were nonlinearly related in a complex way. This method opens up the question of where nonlinear dynamical interdependence could identify new functional relations among the nervous system.

The nonlinear cross-prediction method is closely related to other recent techniques which evaluate the closeness between dynamical systems (for example the normalized cross-correlation sum of [29,30] or cross-prediction error of [31–33]). In these statistics, the purpose is to investigate the similarity between two time series by quantifying a distance between the two underlying *dynamics* or attractors. Thus, these methods sensitively depends on any nonlinear transformation of one data set with respect to the other. Furthermore, the two related time series might be out of phase with each other. In this paper, we investigate a close but different question, the existence of a mapping between the *trajectories* of two reconstructed systems. Here, as illustrated by our numerical example, the functional relationship between pair of signals is directly investigated. Moreover, finding evidence of a dynamical interdependency between two sets implies that their temporal evolutions were "synchronized" even if the interaction is not always characterized by the perfect equality of the variables [17]. Another test in the same context is given by a mutual false nearest neighbor technique developed in [17]. However, this test requires longer segments and a low noise level in order to obtain stable results. It is further well known that global nonlinear predictions with locally constant approximations yield good results for rather short seg-

ments [34,35], and is then much better adapted to the data segmentation of EEG recordings [32,33].

If a function exists that maps the value from one attractor to another, this implies the ability to predict one system through the knowledge of the other [17,21]. This is the case of the situation where a subsystem, X, drives another one, Y, without being strongly influenced by the latter. In fact, the crucial feature is here the ability to completely predict the response Y from an observation of the driver X alone. Thus, by calculating the cross-predictabilities in both directions ($X \rightarrow Y, Y \rightarrow X$) we may obtain some knowledge about the causality between the two systems by the asymmetry of the relationship. These considerations are of practical importance in neurophysiology when one wishes to characterize the relationship between different brain signals. Indeed the type of nonlinear interactions that can be expected between different brain areas is a transfer function with single or double rectification as seen in neuronal membranes. This is a specific case of strong nonlinear function which is not single-valued. In this way, by calculating the cross-predictabilities in both directions between pairs of brain signals, one can expect that the identification of strong values with a large asymmetry can be interpreted as corresponding mainly to an unidirectional coupling.

Nevertheless, two weaknesses of the method should be noted:

1. The cross-prediction does not take account the possibility of a time delay between the driving and responding system. Delay may be expected due to axonal transport and synaptic processes but the existence of considerably longer delays has been demonstrated in the literature, in particular during the spread of epileptiform activity [37]. In the case of a longer delay between two systems (greater than the sampling time, in our recordings of 5 ms), the cross-predictability method may not detect a significant interaction. According to the present work, we propose the following extension of our procedure to take into account the existence of time delay. The nonlinear cross-predictability can be calculated for a range of time shifts τ between pairs of signals, i.e. $\mathrm{Pred}_{X(t+\tau)\rightarrow Y(t)}$ and $\mathrm{Pred}_{Y(t+\tau)\rightarrow X(t)}$. The time shift in which the association value reached a maximum can be used to measure the degree of interdependence, and can also give an estimate of time delay between two EEG signals. The sign of the delay can also be used to gain further knowledge about the causality between the signals [9].
2. The validity of inferring causality from an asymmetry in the cross-prediction must be discussed. In fact, it is extremely difficult in real situations to clearly prove driving influences between two subsystems. A thorough discussion of causality and driving in electrophysiology is given in [38]. A particular ambiguous case is where an association between two systems is induced only by a third system and not by a mutual causality. In this case the mutual predictability may (falsely) detect a driving influence. Nevertheless, in our work we have taken a rather pragmatic point of view and mostly focused our attention on cross-predictabilities in relation to the epileptogenic regions (that are unambiguously localized during the clinical investigations). In this case, entrainments by the focus of other brain regions can be expected. The identification of asymmetries in the cross-predictability provides here a least ambiguous way of characterizing the causality between brain signals. However, further theoretical work to develop the concept of causality using delay coordinate embedding would be useful.

Despite these weaknesses, the usefulness of the proposed nonlinear cross-predictability measure was here confirmed by quantifications of interdependences in intracranial EEGs from patients with temporal lobe epilepsy. Perhaps the most important of our findings is that the epileptogenic region can be distinguished from the more normal areas during interictal periods and without the contribution of epileptic activity. Recurrent drivings of large brain parts were observed to occur in spatio-temporal patterns related to the location of the epileptogenic focus. Furthermore, the comparison with multivariate surrogate data shows that prominent nonlinearities were present in these large-scale entrainments generated by the epileptogenic mesiotemporal structures. This suggests that the process of entrainment coming from the epileptogenic areas involves widespread nonlinear functional linkages toward distant neuronal sources. A similar conclusion is reached by an experimental animal model of epilepsy (limbic kindling) [39,40] that shows the occurrences of transient high nonlinear interactions between neuronal structures. Our results are also con-

sistent with the recent observations by Casdagli et al. [12,13] showing that prominent nonlinearities exist in intracranial EEG recordings generated by the epileptogenic structures during the interictal period and from patients with temporal lobe epilepsy.

For a comparable group of patients, we suggest here that the use of analytic techniques designed to detect and characterize nonlinearities between recording channels may be proved to be useful in detecting epileptogenic foci during interictal periods. Thus the use of the present analysis could be complementary to the visual assessment of the EEG and contribute to improve the accuracy of presurgical diagnostic purpose. These conclusions must of course be verified on a large sample of patients before being applied in a clinical setting. Furthermore, our data are drawn from a well-defined population of patients suffering from medial temporal lobe epilepsy. Our goal was here explicitly to demonstrate the existence and usefulness of nonlinear interdependencies in a model of human epilepsy. But we expect that the functional properties retrieved in this model are applicable to other types of partial epilepsies. Furthermore, it remains to be seen whether or not these techniques can be successfully applied to the analysis of noninvasive (scalp) recordings of the EEG. It is possible that the skull and scalp attenuate or distort (filter out) nonlinearities that are detectable with subdural and depth electrode recordings. These questions will be addressed in further studies.

From a clinical point of view, the observation of recurrent drivings suggests that subtle facilitation of new abnormal pathways of connections from an epileptogenic region can be related with the epileptic process, as has been already suggested in [41]. These facilitations would be present in an intermittent fashion and may perhaps subserve the transition towards a seizure onset. In this perspective, the occurrence of a seizure may not be considered as an abrupt event, but as a phenomenon that emerge from a progressive facilitation of the pathways already seen in interictal periods. This finding raises then the possibility that the detection of subtle recruitment states give insights into the dynamics of the neuronal synchronization before a epileptic seizure, and perhaps may predict the onset of a seizure before its manifestation on the EEG tracings. Indeed, it is notoriously difficult to predict the onset of seizures more than a few seconds in advance from a visual inspection of the EEG. Analyses based on linear autoregressive models [42] also indicate that changes in the EEG may be detectable for few seconds before the actual seizure onset. Our ongoing research is devoted to the characterization of subtle nonlinear pre-seizure neuronal entrainments that would enable the identification of precursors to seizure onset [15,23,43].

Acknowledgements

We thank T. Schreiber, P. Grassberger, K. Lehnertz and J. Müller-Gerking for useful conversations and the reading of the manuscript.

References

[1] D. Lehmann, Principles of spatial analysis, in: A.S. Gevins, A. Rémond (Eds.), Methods of Analysis of Brain Electric and Magnetic Signals, EEG Handbook (revised series, vol. 1), Elsevier, Amsterdam, 1987, pp. 309–354.
[2] G.L. Gerstein, D.H. Perkel, Simultaneously recorded trains of action potentials: Analysis and functional interpretation, Science 164 (1969) 828–830 .
[3] A.R. Damasio, The brain binds entities and events by multiregional activation from convergence zones, Neural Comput. 1 (1989) 123–132.
[4] K.J. Friston, C.D. Frith, R.S.J. Frackowiak, Time-dependent changes in effective connectivity measured with PET, Human Brain Mapping 1 (1993) 69–79.
[5] V. Menon, W.J. Freeman, B.A. Cutillo, J.E. Desmond, M.F. Ward, S.L. Bressler, K.D. Laxer, N. Barbaro, A.S. Gevins, Spatio-temporal correlations in human gamma band electrocorticograms, Electroenceph. Clin. Neurophysiol. 98 (1996) 89–102.
[6] T.H. Bullock, M.C. NcClune, J.T. Achimowicz, V.J. Iragui-Madoz, R.B. Duckrow, S.S. Spencer, EEG coherence has structure in the millimeter domain: subdural and hippocampal recordings from epileptic patients, Electroenceph. Clin. Neurophysiol. 95 (1995) 161–177.
[7] T.M. McKenna, T.A. McMullen, M.F. Shlesinger, The brain as a dynamic physical system, Neuroscience 60 (1994) 587–605.
[8] F.H. Lopes da Silva, J.P. Pijn, EEG analysis. in: M.A. Arbib (Ed.), The Handbook of Brain Theory and Neural Networks, MIT Press, Cambridge, MA, 1995, pp. 348–351.
[9] F.H. Lopes da Silva, J.P Pijn, P. Boeijinga, Interdependence of EEG signals: Linear vs. nonlinear associations and the significance of time delays and phase shifts, Brain Tomography 2 (1989) 9–18.
[10] M. Le Van Quyen, C. Adam, M. Baulac, J. Martinerie, F.J. Varela, Nonlinear interdependences of EEG signals in human intracranially recorded temporal lobe seizures, Brain Res. 792 (1998) 24–40.
[11] S.A.R. Rombouts, R.W.M Keunen, C.J. Stam, Investigation of nonlinear structure in multichannel EEG, Phys. Lett. A 202 (1995) 352–358.

[12] M.C. Casdagli, L.D Iasemidis, J.C. Sackellares, S.N. Roper, R.L. Gilmore, R.S. Savit, Characterizing nonlinearity in invasive EEG recordings from temporal lobe epilepsy, Physica D 99 (1996) 381–399.
[13] M.C. Casdagli, L.D. Iasemidis, R.S. Savit, R.L. Gilmore, S.N. Roper, J.C. Sackellares, Nonlinearity in invasive EEG recordings from patients with temporal lobe epilepsy, Electroenceph. Clin. Neurophysiol. 102 (1997) 98–105.
[14] J.P Pijn, J.V. Neerven, A. Noest, F.H. Lopes da Silva, Chaos or noise in EEG signals: dependence on state and brain site, Electroenceph. clinic. Neurophysiol. 79 (1991) 371–381.
[15] K. Lehnertz, C.E. Elger, Spatio-temporal dynamics of the primary epileptogenic area in the temporal lobe epilepsy characterized by neuronal complexity loss, Electroenceph. Clin. Neurophysiol. 95 (1995) 108–117.
[16] M. Le Van Quyen, J. Martinerie, C. Adam, F. Varela, Unstable periodic orbits in human epileptic activity, Phys. Rev. E 56 (1997) 3401–3411.
[17] N.F. Rulkov, M.M. Sushchik, L.S. Tsimring, H.D.I. Abarbanel, Generalized synchronization of chaos in directionally coupled chaotic system, Phys. Rev. E 51 (1995) 980–994.
[18] S.J. Schiff, P. So, T. Chang, R.E. Burke, T. Sauer, Detecting dynamical interdependence and generalized synchrony through mutual prediction in a neural ensemble, Phys. Rev. E 54 (1996) 6708–6724.
[19] H.D.I. Abarbanel, N.F. Rulkov, M.M. Sushchick, Generalized synchronization of chaos: the auxiliary system approach, Phys. Rev. E 53 (1996) 4528–4535.
[20] L.M. Pecora, T.L. Carroll, J.F. Heagy, Statistics for mathematical properties of maps between time series embeddings, Phys. Rev. E 52 (1995) 3420–3439.
[21] L. Kocarev, U. Parlitz, Generalized synchronization, predictability, and equivalence of unidirectionaly coupled dynamical system, Phys. Rev. Lett. 76 (1996) 1816–1819.
[22] J. Engel, Seizure and Epilepsy, Davis Company, 1989.
[23] L.D. Iasemidis, J.C. Sackellares, H.P. Zaveri, W.J. Williams, Phase space topography and the Lyapunov exponent of electrocorticograms in partial seizures, Brain Topography 2 (1990) 187–201.
[24] M.T. Rosenstein, J.J. Collins, C.J. De Luca, Reconstruction expansion as a geometry-based framework for choosing proper delay times, Physica D 73 (1994) 82–98.
[25] M.B. Kennel, R. Brown, H.D. Abarbanel, Determining minimum embedding dimension using a geometrical construction, Phys. Rev. A 45 (1992) 3403–3411.
[26] C.G. Schroer, T. Sauer, E. Ott, J.A. Yorke, Predicting chaos most of the time from embeddings with self-intersections, Phys. Rev. Lett. 80 (1998) 1410–1413.
[27] J. Theiler, S. Eubank, A. Longtin, B. Galdrikian, J.D. Farmer, Testing for nonlinearity in time series: the method of surrogate data, Physica D 58 (1992) 77–94.
[28] D. Prichard, J. Theiler, Generating surrogate data for the time series with several simultaneously measured variables, Phys. Rev. Lett. 73 (1994) 951–955.
[29] H. Kantz, Quantifying the closeness of fractal measures, Phys. Rev. E 49 (1994) 5091–5097.
[30] R. Manuca, R. Savit, Stationarity and nonstationarity in time series analysis, Physica D 99 (1996) 134–161.
[31] J.L. Hernandez, R. Biscay, J.C. Jimenez, P. Valdes, R.R. Grave de Peralta, Measuring the dissimilarity between EEG recordings through a nonlinear dynamical system approach, Int. J. Bio-Med. Comput. 38 (1995) 121–129.
[32] T. Schreiber, Detecting and analysing nonstationarity in a time series using nonlinear cross predictions, Phys. Rev. Lett. 78 (1997) 843–846.
[33] T. Screiber, A. Schmitz, Classification of time series data with nonlinear similarity measures, Phys. Rev. Lett. 79 (1997) 1475–1478.
[34] G. Sugihara, R.M. May, Nonlinear forecasting as a way of distinguishing chaos from measurement error in a data series, Nature 344 (1990) 734–741.
[35] M. Castagli, Nonlinear prediction of chaotic time series, Physica D 35 (1989) 335–356.
[36] F.J. Varela, Resonant cell assemblies: a new approach to cognitive functions and neuronal synchrony, Biol. Res. 28 (1995) 81–95.
[37] J. Gotman, Measurement of small time differences between EEG channels: methods and application to epileptic seizure propagation, Electroenceph. clinic. Neurophysiol. 56 (1983) 501–514.
[38] W. Gersch, Causality or driving in electrophyiological signal analysis, Math. Biosci. 14 (1972) 177–196.
[39] N.J. Mars, F.H. Lopes da Silva, Propagation of seizure activity in kindled dogs, Electroenceph. clinic. Neurophysiol. 56 (1983) 194–209.
[40] H.J. Beldhuis, T. Suzuki, J.P. Pijn, A. Teisman, F.H. Lopes da Silva, B. Bohus, Propagation of epileptiform activity during development of amygdaka kindling in rats: linear and non-linear association between ipsi-and contralateral sites, Eur. J. Neurosci. 5 (1993) 944–954.
[41] P. Buser, J. Bancaud, Unilateral connections between amygdala abd hyppocampus in man. A study of epileptic patients with depth electrodes, Electroenceph. clinic. Neurophysiol. 55 (1983) 1–12.
[42] Z. Rogowski, I. Gath, E. Bental, On the prediction of epileptic seizures, Biol. Cybern. 42 (1981) 9–15.
[43] J. Martinerie, C. Adam, M. Le Van Quyen, M. Baulac, S. Clemenceau, B. Renault, F.J. Varela, Epileptic seizure can be anticipated by nonlinear analysis, Nature 4 (1998) 1173 .